



Transport and environmental temperature variability of eggs and larvae of the Japanese anchovy (*Engraulis japonicus*) and Japanese sardine (*Sardinops melanostictus*) in the western North Pacific estimated via numerical particle-tracking experiments

SACHIIHIKO ITOH,^{1,*} ICHIRO YASUDA,¹
HARUKA NISHIKAWA,¹ HIDEHARU
SASAKI,² AND YOSHIKAZU SASAI³

¹Ocean Research Institute, The University of Tokyo, 1-15-1,
Minamidai, Nakano-ku, Tokyo 164-8639, Japan

²Earth Simulator Center, Japan Agency for Marine-Earth
Science and Technology, 3173-25, Showa-machi, Kanazawa-
ku, Yokohama 236-0001, Japan

³Frontier Research Center for Global Change, Japan Agency for
Marine-Earth Science and Technology, 3173-25, Showa-machi,
Kanazawa-ku, Yokohama 236-0001, Japan

ABSTRACT

Numerical particle-tracking experiments were performed to investigate the transport and variability in environmental temperature experienced by eggs and larvae of Pacific stocks of the Japanese anchovy (*Engraulis japonicus*) and Japanese sardine (*Sardinops melanostictus*) using high-resolution outputs of the Ocean General Circulation Model for the Earth Simulator (OFES) and the observed distributions of eggs collected from 1978 to 2004. The modeled anchovy individuals tend to be trapped in coastal waters or transported to the Kuroshio–Oyashio transition region. In contrast, a large proportion of the sardines are transported to the Kuroshio Extension. The egg density-weighted mean environmental temperature until day 30 of the experiment was 20–24°C for the anchovy and 17–20°C for the sardine, which can be explained by spawning areas and seasons, and interannual oceanic variability. Regression analyses revealed that the contribution of environmental temperature to the logarithm of recruitment per spawning (expected to have a negative relationship

with the mean mortality coefficient) was significant for both the anchovy and sardine, especially until day 30, which can be regarded as the initial stages of their life cycles. The relationship was quadratic for the anchovy, with an optimal temperature of 21–22°C, and linear for the sardine, with a negative coefficient. Differences in habitat areas and temperature responses between the sardine and anchovy are suggested to be important factors in controlling the dramatic out-of-phase fluctuations of these species.

Key words: Japanese anchovy, Japanese sardine, particle-tracking experiment

INTRODUCTION

The Japanese anchovy (*Engraulis japonicus*) and Japanese sardine (*Sardinops melanostictus*) are two of the most abundant and commercially important pelagic species in the western North Pacific. Their spawning grounds are mainly formed in the temperate southern and eastern waters of the Japanese Islands. The feeding grounds of juveniles and adults are found across wide regions of the Kuroshio Extension and the Kuroshio–Oyashio transition region, east of Japan (Fig. 1).

The stock abundances of these two species show dramatic out-of-phase fluctuations on a multidecadal time scale (Fig. 2a). Based on total commercial landing data in Japanese waters (Yatsu *et al.*, 2005; note that although these data include the contribution of all stocks in Japanese waters, they are considered to represent the fluctuation trend of the Pacific stocks because these stocks are generally the most abundant), anchovy stocks were high in the 1910–20s, 1950–60s, and 1990–2000s, whereas sardine stocks showed the opposite trend. The same patterns of anchovy and sardine regime shifts were observed in the California Current and Humboldt Current systems, and a relationship with climatic regime shift has been suggested (Lluch-Belda *et al.*, 1989; Kawasaki, 1991; Chavez

*Correspondence. e-mail: itohsach@ori.u-tokyo.ac.jp

Received 13 May 2008

Revised version accepted 26 December 2008

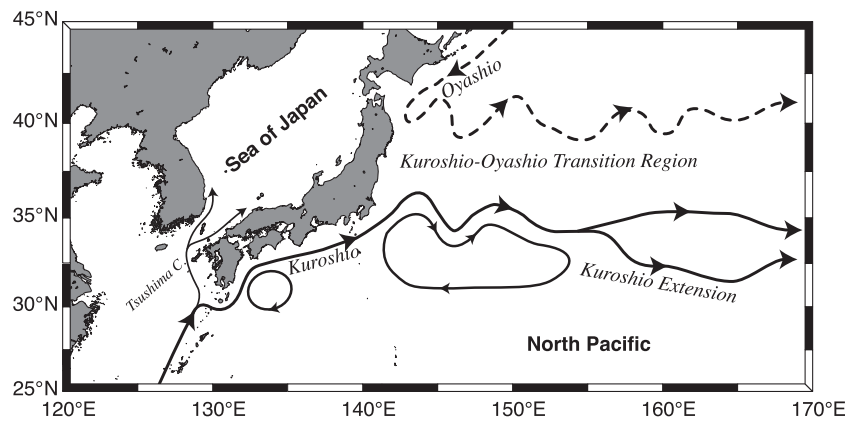


Figure 1. Simplified hydrography of the western North Pacific.

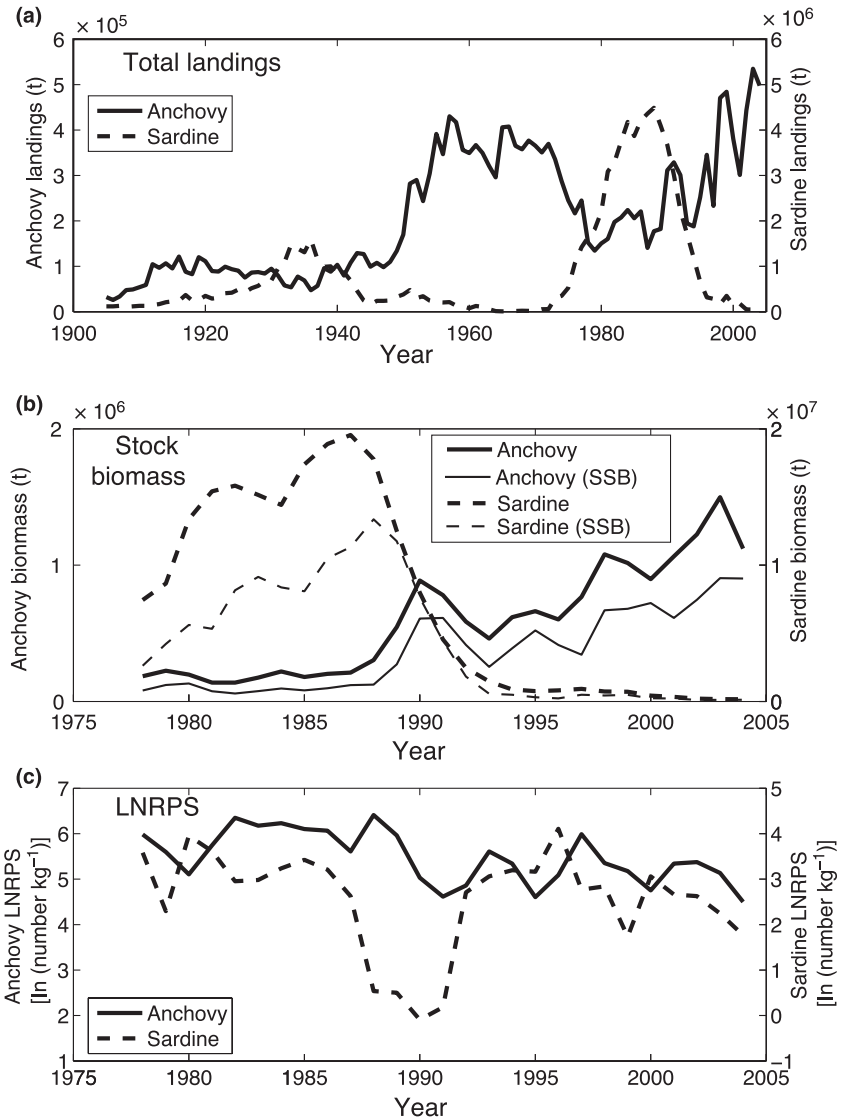


Figure 2. Interannual variations in (a) total landings in Japanese waters from historical data (updated from Yatsu *et al.*, 2005), (b) stock abundance and spawning stock biomass (SSB), and (c) logarithms of recruitment per spawning biomass (LNRPS) for the Japanese anchovy and Japanese sardine.

et al., 2003); however, decadal variability in upper-layer temperatures shows contrasting trends in the eastern and western North Pacific (Mantua *et al.*, 1997). The sardine regime corresponds to the cold period in the west (Yasuda *et al.*, 1999) and the warm period in the east (Hare and Mantua, 2000; Chavez *et al.*, 2003).

Although there are several major stock groups of the Japanese anchovy and Japanese sardine, based on their adult habitats (i.e., the Pacific, the Tsushima warm current, and the Seto Inland Sea), interannual fluctuations in their abundances show the same patterns among the different groups. Therefore, this study considers the Pacific stocks, which are generally the most abundant.

It has been confirmed from recent records of stock abundances and recruitment rates that these fluctuations in abundance are mainly caused by recruitment variability. Watanabe *et al.* (1995) found that the survival rates of 1-yr individuals of the Japanese sardine were extremely low in 1988–90 when the sardine stock was rapidly decreasing; this did not occur instantaneously at the ‘critical period’ (Hjort, 1914) but cumulatively throughout their early life stages. Comparing the fluctuations in stock abundance and recruitment per spawning biomass (RPS) over the past 30 yr, we observe a major influence of RPS on a trend of stock, with a 1-yr lag, for both the Japanese anchovy (e.g., RPS peak in 1988 and stock increase in 1988–89, and RPS trough in 1991 and stock decrease in 1991–92) and Japanese sardine (e.g., high RPS in 1984–86 and stock increase in 1984–87, and low RPS in 1988–91 and stock decreases in 1988–92; Fig. 2b,c). Although the stock abundance of sardine has been extremely low since 1993, the above correspondence is still observed if we consider the stock fluctuation ratio $(S_{i+1} - S_i)/S_i$, where S_t is stock abundance in year i (not shown in the figure).

Because the spawning grounds extend from inshore areas to the Kuroshio areas, especially when the stock abundances are high (Watanabe *et al.*, 1996), large numbers of larvae are expected to be transported to the Kuroshio Extension (Heath *et al.*, 1998); indeed, anchovy and sardine larvae have been collected from this area in the past (Sugisaki, 1996; Nagasawa and Davis, 1998). Using simple analytical and numerical models, Kasai *et al.* (1992) identified a correlation between survival rates and retention rates around spawning areas for sardine larvae after 1 month from hatching; however, the results obtained from a similar numerical model (but including eastern offshore areas of Japan) indicated that the abundances of sardine juveniles transported to the eastern offshore areas of

Japan make a major contribution to recruitment (Kasai *et al.*, 1997). Noto and Yasuda (1999) were the first to document a significant positive correlation between the mortality coefficient of sardine larvae and winter sea-surface temperatures (SST) in the Kuroshio Extension and its southern recirculation areas (KESA), based on data for the period 1979–94.

The logarithm of RPS (herein referred to as LNRPS) is expected to show a relationship with survival through the stages from egg to recruitment. Yatsu *et al.* (2005) reported that the density effect together with SST in KESA explained about 40% of the variability in LNRPS of sardine from 1950 to 2000 ($R^2 = 0.37$, $P < 0.01$). Nishikawa and Yasuda (2008) suggested that fluctuations in the timing of the spring bloom caused by mixed-layer variability in KESA is related to the survival of sardine larvae that might be transported to this site; however, this hypothesis is unable to explain fluctuations in the anchovy population, which is assumed to be distributed in the same region and mainly feeds on the same food (copepods) as sardine during its early life stages.

Takasuka *et al.* (2007) proposed a hypothesis of optimal growth temperature, which seeks to explain stock fluctuations in the anchovy and sardine in terms of environmental temperature by analyzing the otolith microstructure of the larvae of each species. The optimal temperature for larval growth is 22.0°C for the anchovy and 16.2°C for the sardine, thereby explaining the anchovy and sardine regimes in warm and cold periods, respectively. This finding also suggests that the optimal temperature hypothesis is valid for the California anchovy and California sardine in the region of the California current system, because the representative spawning temperature is significantly lower for anchovy than for sardine, consistent with the anchovy (sardine) regime in cold (warm) periods (Takasuka *et al.*, 2008). However, a retrospective analysis of the Japanese anchovy and Japanese sardine, using spawning ground temperature, failed to provide a significant explanation of RPS variability, especially for sardine (Takasuka *et al.*, 2007).

The results of the above studies suggest the importance of temperature in larval survival and subsequent recruitment; however, the temperature data used in these studies were obtained from either fixed areas or spawning grounds. Because some larvae are expected to be entrained in the Kuroshio current from inshore waters and to be transported to the Kuroshio Extension, the effect of Lagrangian temperature variability cannot be neglected; however, data based on observations are limited. Itoh and Kimura (2007) analyzed drifter data collected by the World Ocean

Circulation Experiment–Surface Velocity Program (WOCE–SVP) and described the characteristics of transport and Lagrangian temperature variability; however, few data are available before 1990, when a dramatic fluctuation in stock occurred.

The recently developed Ocean General Circulation Model for the Earth Simulator (OFES) covers almost the entire globe at a horizontal resolution of 0.1° and with 54 vertical levels (Masumoto *et al.*, 2004). Unlike the simple models used in previous studies (Kasai *et al.*, 1992, 1997), which describe flows of the Kuroshio via constant inflow/outflow, OFES is driven by realistic atmospheric forcing (including temporal and spatial variability), and hydrographic fields are reproduced via appropriate governing equations. A hindcast integration performed using this model for the years 1950–2004 (Sasaki *et al.*, 2008) reproduces well the decadal upper-layer variability in the western North Pacific (Nonaka *et al.*, 2006; Taguchi *et al.*, 2007). The typical SST fluctuation pattern of the mid- and high-latitude North Pacific, as represented by empirical orthogonal functions (EOF) [known as Pacific Decadal Oscillation, (PDO), Mantua *et al.*, 1997], is also well reproduced in EOFs using the modeled SST (Sasaki *et al.*, 2008). We used the outputs from this model for our numerical particle-tracking experiments.

The main purpose of this study is to demonstrate interannual variability in the transport of larvae of the Pacific stocks of the Japanese anchovy and Japanese sardine (herein referred to as anchovy and sardine, respectively) and the Lagrangian temperature variability experienced by these species over the past 30 yr, for which spawning-ground data are available, using more realistic data and procedures than those adopted in previous, simple models (Kasai *et al.*, 1992, 1997) or statistical analyses (Noto and Yasuda, 1999; Yatsu *et al.*, 2005). We also examine various hypotheses regarding the survival of these species, as proposed in previous studies.

MATERIALS AND METHODS

OFES hindcasts and particle release points

Horizontal velocity, temperature, and mixed layer depth (snapshots at 3-day intervals) in the upper 1000 m of the western North Pacific were hindcasted for the years 1950–2004; data for the period 1978–2004 were used in the particle tracking experiments (Fig. 3a). By using the snapshot data of 3-day intervals instead of averaged data for longer periods (e.g., monthly means), we could implicitly include a greater component of dispersion effects in the advection

process, meaning that they were less dependent on diffusivity parameterized via horizontal velocity data. Ten particles were released from $30' \times 30'$ grids in the areas shown in Fig. 3b (which covers the spawning areas of anchovy and sardine) on the 16th of each month (not representing eggs at this time; see the following paragraphs for weighting procedures regarding observed monthly egg production). Their movement and Lagrangian environmental variability were tracked for 90 days, the period approximately covering larval stages; longer tracking periods have less meaning, as the swimming ability of juveniles is not negligible.

The transport and environments of the eggs and larvae were estimated by weighting the particles with the observed egg densities at their initial locations. Although OFES is generally successful in reproducing the upper-layer hydrographic features of the western North Pacific (Nonaka *et al.*, 2006; Taguchi *et al.*, 2007), the temporal variability in highly nonlinear processes such as path variations in the Kuroshio and the pinch-off of warm and cold core rings does not always coincide with observations. In such a case, weighting based on latitude and longitude may yield an incorrect description of the transport, because slight differences in the modeled path of the Kuroshio cause large differences in the destinations of the eggs and larvae distributed around the actual path of the Kuroshio.

To avoid this problem, we divided the waters south and east of Japan, covering the spawning areas, into eight areas (SA1–SA8) based on water depth and the location of the Kuroshio axis (Fig. 3b). The water south of Japan, $130\text{--}145^\circ\text{E}$ and $28\text{--}36^\circ\text{N}$, including the southeastern part of the East China Sea, was divided into eastern and western parts according to the $135^\circ30'\text{E}$ line, and each part was divided into three areas: coastal, inshore, and offshore. The coastal and inshore areas were distinguished by water depth (deeper or shallower than 200 m, based on a model grid of 208 m depth), and the inshore and offshore areas were divided by the axis of the Kuroshio current, defined by 200-m temperatures (Kawai, 1969) of 15°C for the eastern part and 16.5°C for the western (using the model temperature at a depth of 208 m), which also worked well in the model, especially in dividing $30' \times 30'$ particle-releasing grids. Because eggs are not found in offshore waters far from the axis of the Kuroshio, the southern boundaries of the offshore areas were assumed to be those lines whose magnitude of velocity was $>0.5 \text{ m s}^{-1}$ at a depth of 2.5 m (the shallowest grid). Therefore, the offshore areas south of Japan were the same as the areas around the axis of the

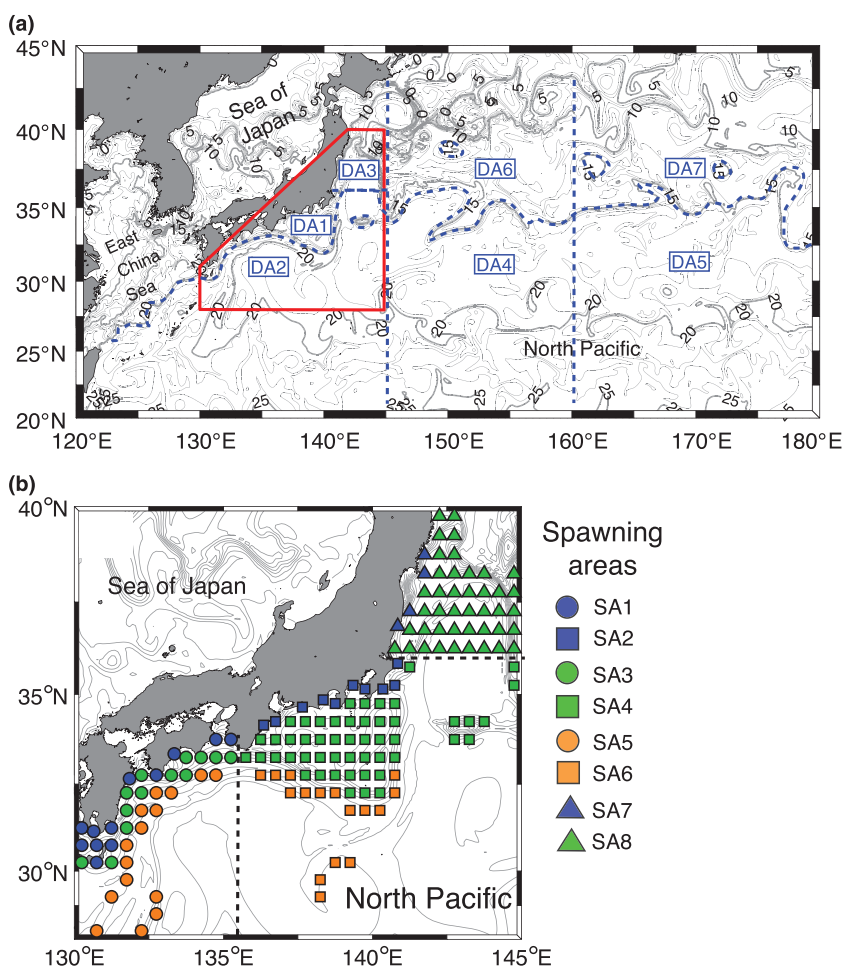


Figure 3. (a) Domain of the particle-tracking experiments: model spawning areas (particle release areas) and destination areas (DA1–DA7) are shown with thick red solid lines and thick blue dashed lines, respectively. The background thin gray lines are temperature contours (contour interval, 2.5 m) for 16 February 1985, as calculated by OFES. (b) Model spawning grounds (SA) in February 1985, showing the distributions of particles determined by the criteria described in the text. The thin gray lines are as in (a).

Kuroshio current (Kuroshio areas). The water east of Japan, 36–40°N and west of 145°E, was divided into coastal and inshore areas based on a water depth of 200 m (model grid of 208 m). Furthermore, areas with SST below 11°C and above 30°C, where few anchovy or sardine eggs are found, were eliminated each month. Thus, we considered six areas south of Japan and two east of Japan, including 153–253 particle-release points.

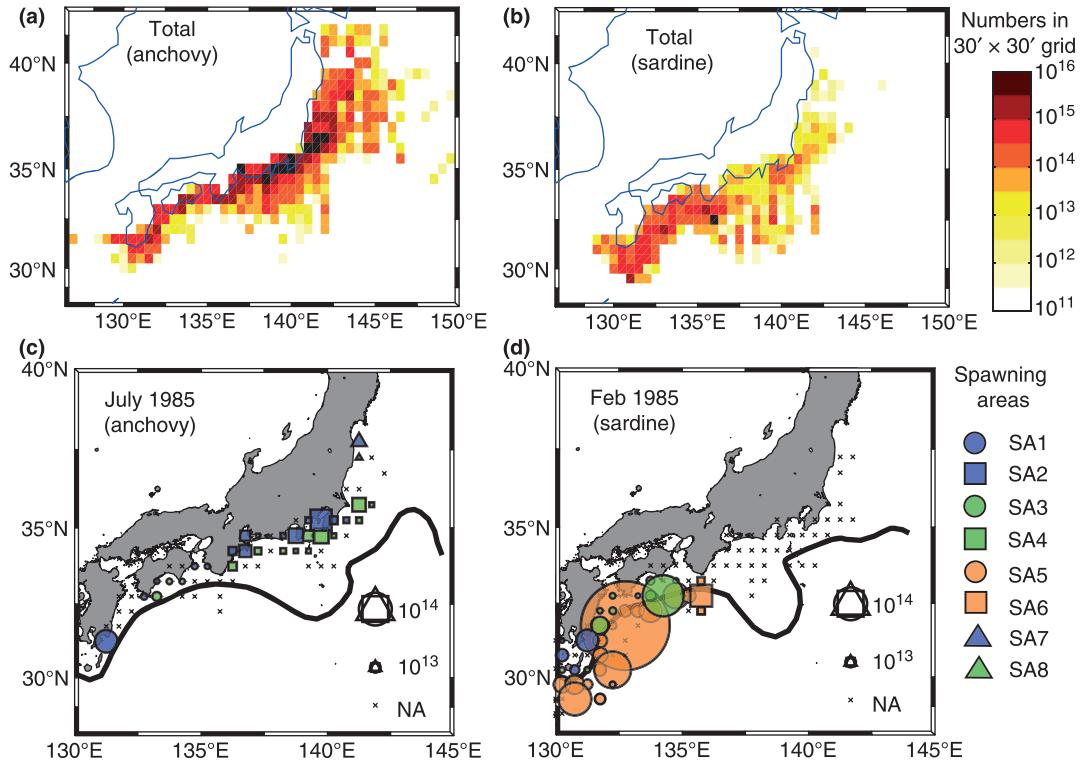
Egg distributions based on observations

Egg abundance data for the Japanese sardine and Japanese anchovy along the Pacific coast of Japan are collected, processed, and archived by the Fisheries Research Agency of Japan (Mori *et al.*, 1988; Kikuchi and Konishi, 1990; Ishida and Kikuchi, 1992; Zenitani *et al.*, 1995; Anonymous, 1997–2004; Kubota *et al.*, 1999).

The data from a 30' × 30' grid, collected from 1978 to 2004, were used to weight our particle-tracking experiments. Figure 4a,b shows the observed distribu-

tion of the sum of egg abundances from 1978 to 2004. Dense egg abundances for the anchovy were found in inshore areas south and east of Japan, whereas those of the sardine were found in the Kuroshio area, south of Japan, especially in the western part. These spawning grounds were then divided into eight areas, as in the model. The same divisions as those used in the model were applied to the coastal and inshore areas for waters both south and east of Japan, considering the latitude, longitude, and water depth. However, the axis of the Kuroshio, which divides the inshore and offshore areas, was taken from data provided by the Marine Information Research Center (2007), which archives the comprehensive observations made by the Japan Coast Guard. These data included both thermal and current structures rather than the 200 m temperatures, which were not always obtained with sufficient spatial coverage. Examples for February 1985 for the sardine and July 1985 for the anchovy are shown in Fig. 4c,d, respectively.

Figure 4. Sums of estimated egg abundances (numbers in a $30' \times 30'$ grid) for (a) anchovy and (b) sardine in the western North Pacific from 1978 to 2004, based on observations (see text for references), and examples of monthly egg abundances for (c) anchovy in July 1985 and (d) sardine in February 1985. Thick black lines in (c) and (d) indicate the path of the Kuroshio current, as taken from Marine Information Research Center (2007).



Particle tracking, egg density-weighted mean environmental temperature, and regression analysis

The movement and environmental variability of all particles in the eight areas of the model were calculated for 90 days at the start of each month from January 1978 to October 2004 (321 measurements). The horizontal movement of the particles was calculated with advection and diffusion terms using the leapfrog scheme:

$$x_{n+1} = x_{n-1} + u_n \Delta t + l_n^x \quad (1)$$

$$y_{n+1} = y_{n-1} + v_n \Delta t + l_n^y \quad (2)$$

where x_n and y_n are the position of a particle at the n th time step; u_n and v_n are the eastward and northward velocity components, respectively, linearly interpolated at x_n , y_n , and z_n (where z_n is the vertical position, as described below) at the corresponding time; $\Delta t = 20$ min is double the time interval; and l_n^x and l_n^y are the eastward and northward steps of a random walk, respectively. Note that the Asselin filter (Asselin, 1972)

was used to update $n - 1$ locations to avoid the splitting generally caused by the leapfrog scheme:

$$x_{n-1} = x_n + 0.1 \times (x_{n-1} - 2x_n + x_{n+1}) \quad (3)$$

The vertical positions were aligned to the middle of the mixed layer depth, defined as that at which the density is increased $0.125 \rho_0$ from the surface (one of the OFES outputs), considering the diurnal vertical migration of the larvae in mixed layers. Other scenarios at fixed depths did not change the general results, unless the depth was deeper than the mixed layers.

The random walk steps are given by

$$(l_n^x, l_n^y) = P_N \sqrt{2\Delta t} \left(\sqrt{A_H^x}, \sqrt{A_H^y} \right) \quad (4)$$

where P_N is a probability function of the normal distribution and A_H^x and A_H^y are variables that depend on the diffusivity coefficients. Whereas constant diffusivity simply gives $A_H^x = A_H^y = A_H$, we estimated these variables from the biharmonic diffusivity terms used in OFES as

$$A_H^x = \min(-B_H \nabla^4 u / \nabla^2 u, 2000) \quad (5)$$

$$A_H^y = \min(-B_H \nabla^4 v / \nabla^2 v, 2000) \quad (6)$$

where $B_H = -27 \times 10^{-9} \text{ m}^4 \text{ s}^{-1}$ is a biharmonic diffusivity constant, and ∇^4 and ∇^2 are the biharmonic and Laplacian operators, respectively. The temperature and mixed layer depth at the particle locations were determined by interpolating the temperature and mixed layer depth data of the OFES outputs.

Spatial distributions were obtained by converting the particle trajectories to numbers in Eulerian grid boxes or seven destination areas (DA1–DA7; Fig. 3a). DA1, DA2, and DA3 were basically merged areas of SA1–SA4 (coastal and inshore areas south of Japan), SA5–SA6 (offshore areas south of Japan), and SA7–SA8 (inshore areas east of Japan), respectively; the SST limitation in the spawning grounds (11–30°C) and the southern boundary of the Kuroshio ($>0.5 \text{ m s}^{-1}$) were not applied. DA4–DA7 were eastern offshore areas divided by the current axis of the Kuroshio Extension (200 m, 14°C; Kawai, 1969) and a meridional line at 160°E.

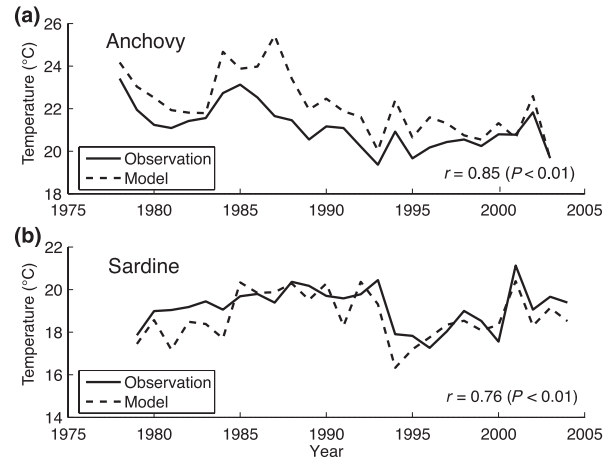
The numbers of particles were weighted according to egg abundance in the corresponding year, month, and area. The egg density-weighted mean environmental temperature (EWMET) and the distribution of individuals, $\langle T(t) \rangle$ and $\langle N(x, y, t) \rangle$, were then obtained as

$$\langle T(t) \rangle_i = \frac{\sum_{jk} e_{ijk} T_{ijk}(t)}{\sum_{jk} e_{ijk}} \quad (7)$$

$$\langle N(x, y, t) \rangle_i = \frac{\sum_{jk} e_{ijk} n_{ijk}(x, y, t)}{\sum_{jk} e_{ijk}} \quad (8)$$

where e_{ijk} denotes egg abundance in spawning area k in year i and month j ; $T_{ijk}(t)$ is the mean environmental temperature of particles from spawning area k in year i and month j at elapsed days t since release; and $n_{ijk}(x, y, t)$ is the normalized density of particles (spatial integration becomes one) at the location (x, y) from spawning area k in year i and month j at elapsed days t since release. Note that the range of sardine spawning in 1 yr is defined from October of the previous year to September of that year, whereas the range for the anchovy is defined from January to December. Although the above equations give annual values averaged over j (months) and k (areas), the weighted means procedure can be conducted over any subscript;

Figure 5. Interannual variations in weighted mean surface temperatures, observed and under initial model conditions, for (a) anchovy and (b) sardine. Correlation coefficients and significance levels are shown in each panel.



if averaging over spawning areas is not conducted, values are obtained for each spawning area separately. As shown in Fig. 5, the initial particle distributions and weighted mean methods were able to accurately reproduce the interannual environment variability of spawning grounds, whereas the base levels were slightly different. Mean differences of +1.0°C for the anchovy and -0.34°C for sardine were subtracted from the environmental temperature for each individual.

The impact of EWMET on LNRPS was examined using regression analysis together with spawning stock biomass (SSB), which generally causes a negative feedback on recruitment. LNRPS and SSB data were taken from the stock assessment reports by Oozeki *et al.* (2005) for anchovy and those by Nishida (2005) for sardine. Linear or quadratic functions of EWMET in any 1 of 19 elapsed day bands, which averaged 11 elapsed days (days 0–10, 5–15, ..., 85–90), were assumed to be $a \langle T(t) \rangle + b$ or $a \langle (T(t) - T_o)^2 \rangle + b$, where T_o is the optimal temperature. Note that the weighted mean of the square product of the environmental temperature $\langle T^2 \rangle$ was needed in addition to EWMET $\langle T \rangle$ to examine the quadratic functions. Although we first used EWMET of individuals from all months and areas (EWMET-ALL: $\langle T \rangle_i$ in Equation 7) for the analyses without SSB, those from each spawning area (EWMET-SA: $\langle T \rangle_{ik}$ without averaging over k in Equation 7) were also examined for the analyses with SSB because EWMET-ALL correlated significantly with SSB. The cause of this correlation and the interpretation of the regression using EWMET-SA are given in the Results,

Discussion and Conclusions section. The significances of the regressions and partial regression coefficients were tested using the *F* test and *t* test, respectively, at a significance level of *P* = 0.1, as in Yatsu *et al.* (2005).

RESULTS

Egg distribution and transport variability

Figure 6 shows interannual fluctuations in the observed egg abundance for anchovy and sardine. The magnitude of variations was extremely high for both species, approximately one order of magnitude for anchovy and two orders of magnitude for sardine (Fig. 6a). As seen in the geographical distributions, large numbers of eggs were spawned in SA2, SA4, and SA8 by anchovy, and in SA1, SA3, SA5, and SA6 by

sardine. The spawning grounds generally expanded with increasing egg abundance. Whereas sardine exhibited marked offshore expansion from SA1–SA2 to SA3–SA6, as shown by Watanabe *et al.* (1996), anchovy showed a northward expansion from SA1–SA2 to SA8.

Interannual variations in the spawning months of anchovy and sardine are shown in Fig. 7. Spawning generally occurs from March to September for anchovy, and from December to April for sardine. Whereas a concentration of spawning in February was observed for sardine with increasing stock abundance, the main spawning season of anchovy became slightly earlier, moving from July to June (Fig. 7).

The destinations of the oceanic current transport show clear differences between the two species,

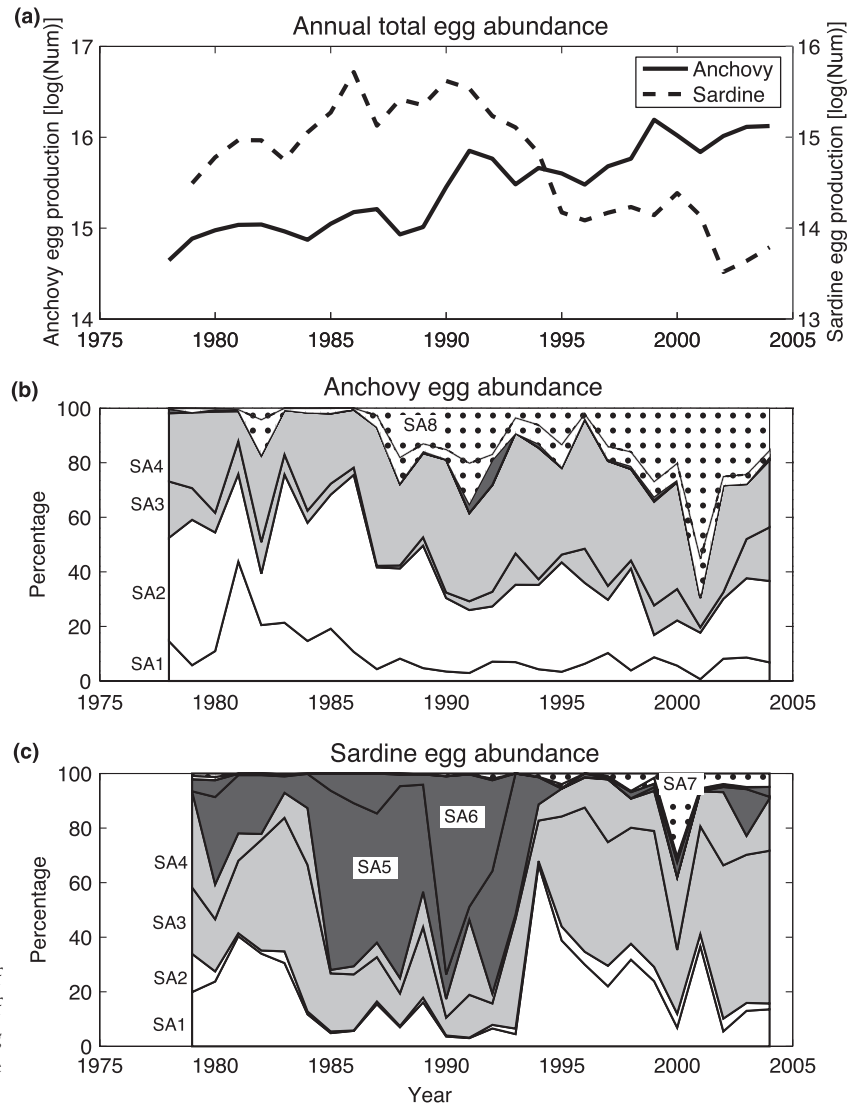
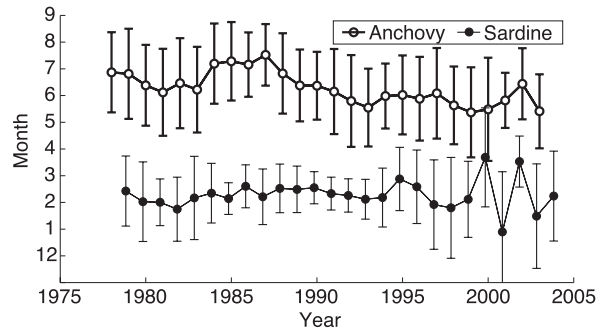


Figure 6. Interannual variations in (a) the annual total egg abundance of anchovy and sardine, (b) proportion of anchovy egg abundance by spawning area (SA), and (c) proportion of sardine egg abundance by SA.

Figure 7. Interannual variations (means and standard deviations) in the spawning months of anchovy and sardine. Note that sardine spawning months in 1 yr are defined from October of the previous year to September of that year.



reflecting differences in spawning grounds (Fig. 8). Offshore transport was more dominant for sardine than for anchovy. Moreover, the destination of the offshore transport was mainly toward the Kuroshio–Oyashio transition region for anchovy, and toward the Kuroshio Extension region for sardine. Because the largest numbers of sardine eggs were spawned in SA5 (Fig. 6a,c), the western part of the Kuroshio area, it is expected that they made a major contribution to the dense distribution of sardines in the Kuroshio Extension region (around 145–155°E) on day 30 (Fig. 8c). This interpretation is consistent with a previous study that observed transport from this area over a distance of 800–900 km in 30 days (Itoh and Kimura, 2007).

Interannual fluctuations in the abundances transported to the destination areas are shown in Fig. 9. Offshore transport tended to increase with increasing stock (egg) abundances for both anchovy and sardine. Anchovy transport to DA1 accounted for more than 50% (30%) of the particles released from the spawning grounds at day 30 (day 90) at the end of the 1970s, whereas it decreased to about 20–40% (10–20%) after the late 1980s, to be replaced especially by transport to DA6. Similarly, sardine transport to DA2 and DA4 in the late 1980s and early 1990s was about 50–70% (40–60%) of the particles released from the spawning grounds, but decreased after the mid 1990s to about 15–30% (10–25%). Transport of anchovy (sardine) to areas east of 160°E (DA5 and DA7) was low on day 30, but by day 90 had increased to about 10–40% (5–30%). Although Kasai *et al.* (1992) suggested a relationship between retention rates within coastal areas and survival rates, the transport ratio to DA1 did not show a significant correlation with RPS for sardine ($r = 0.27$, $P = 0.19$).

Variability of environmental temperatures

The environmental temperatures experienced by the two species can also be compared (Fig. 10). The temperature during the initial stages, until day 30, was about 20–24°C for anchovy and 17–20°C for sardine. This difference is primarily attributable to the difference in the spawning season: June–July for the anchovy and February–March for the sardine (Fig. 7). Conversely, the temperature variability until

Figure 8. Densities of model individuals of (a) anchovy on day 30, (b) anchovy on day 90, (c) sardine on day 30, and (d) sardine on day 90 in 30' × 30' grids estimated by weighted mean densities of all the released particles after the same number of days had elapsed. Destination areas (DAs) are approximately delineated by solid and dashed black lines.

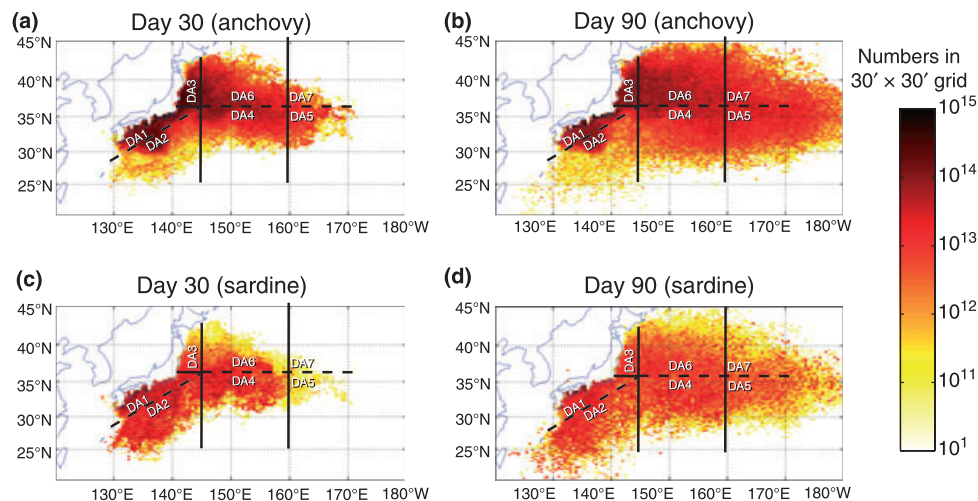
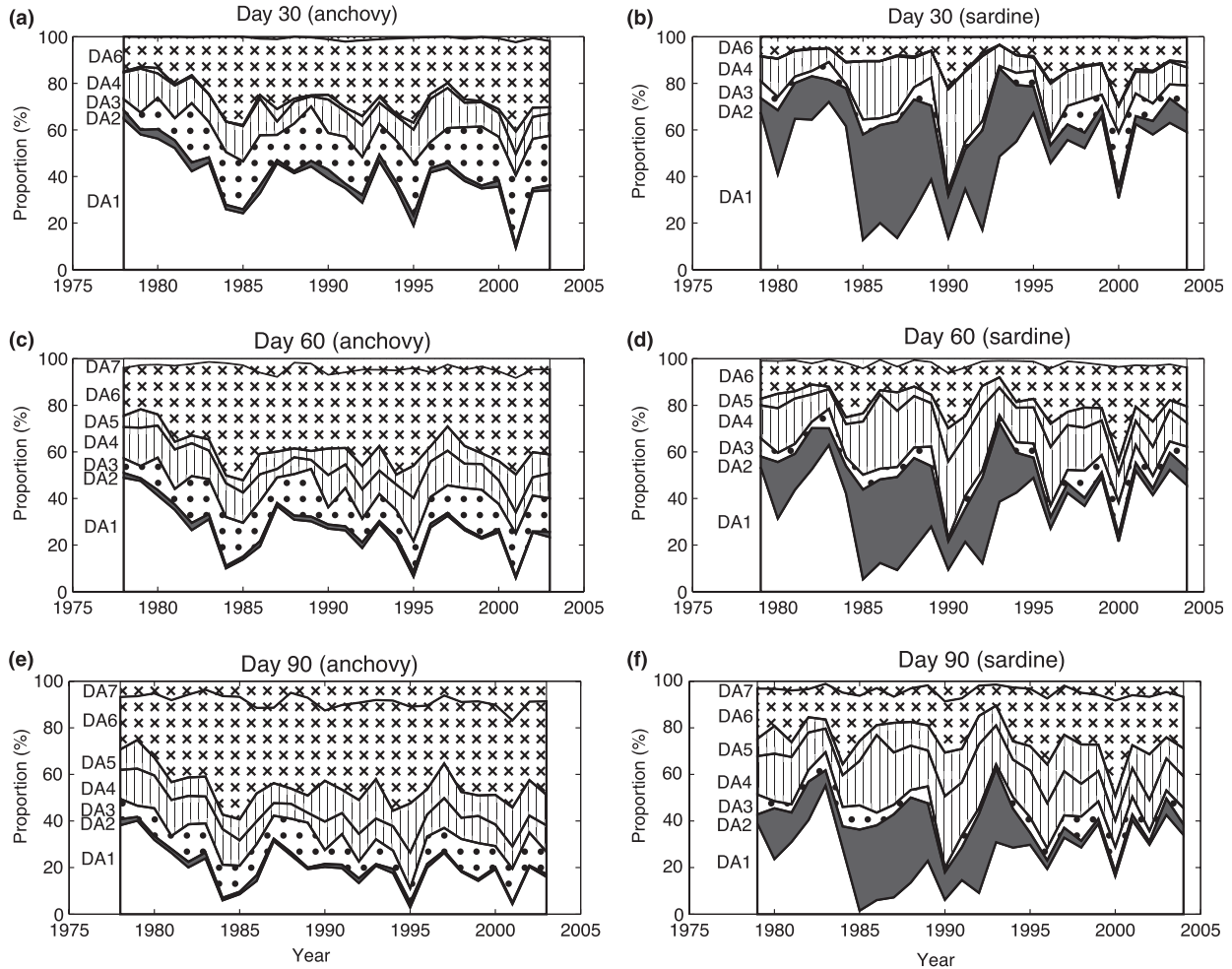


Figure 9. Interannual variations in the proportion of individuals transported to each destination area: (a) anchovy on day 30, (b) anchovy on day 60, (c) anchovy on day 90, (d) sardine on day 30, (e) sardine on day 60, and (f) sardine on day 90.



day 30 for each species is attributed to the expansion, contraction, and movement of the spawning grounds, and fluctuations in the timing of the spawning season (Fig. 10a).

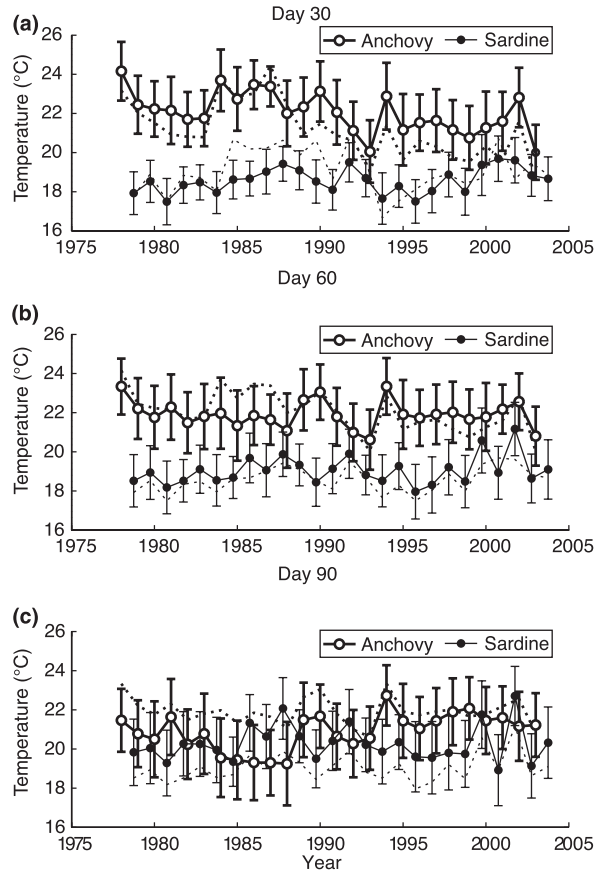
The environment of anchovy during its initial stages has tended to become colder since the end of the 1980s because the spawning grounds have expanded northward and the main spawning season has moved from July to June. The warmer conditions for sardine in the late 1980s and early 1990s are explained by expansion of the spawning ground into the Kuroshio area. A large component of the intra-annual variations can be explained by seasonality: the tendency to warming until day 30 and cooling after day 60 for anchovy, which spawns mainly in the summer, and the tendency to cooling until day 30 and warming after day 60 for sardine, which spawns mainly in February.

Our analysis reveals that spawning variability has a major influence on the transport and environmental temperature fluctuations of the eggs and larvae of anchovy and sardine; however, oceanic variability is also important. The decrease in cooling during the first 30 days for sardine at the end of the 1980s (Fig. 10a), except for 1990, is considered related to the Pacific Decadal Oscillation (Mantua *et al.*, 1997), which in turn is possibly related to the stock collapse reported by Noto and Yasuda (1999). Temperature variations between other stages also differed from year to year, indicating different heating and cooling tendencies.

Relationship between EWMET and RPS

The impact of EWMET on the interannual variability of LNRPS was examined by linear regression analysis (Table 1). We first found a significant regression for

Figure 10. Interannual variations in mean environmental temperatures of model anchovy and sardine individuals on (a) day 30, (b) day 60, and (c) day 90, with half standard deviations shown as error bars, as estimated by weighted average. For comparison, mean environmental temperatures for 30 days before the specified day [i.e., day 0 for (a), day 30 for (b), and day 60 for (c)] are shown by broken lines (thick for anchovy and thin for sardine).



LNRPS using linear functions for EWMET. Anchovy survival increased with increasing EWMET on days 0–10 ($R^2 = 0.20$, $P = 0.02$), whereas sardine survival

decreased with increasing EWMET on days 0–10 ($R^2 = 0.12$, $P = 0.08$). For anchovy, a significant positive relationship was also found after days 0–10 until days 30–40 ($R^2 = 0.12$, $P = 0.08$), with a decreasing trend, and a significant negative relationship was found from days 75–85 ($R^2 = 0.12$, $P = 0.08$) to days 80–90 ($R^2 = 0.16$, $P = 0.05$); however, no day bands other than days 0–10 showed a significant relationship for sardine.

These results, obtained from regressions using linear functions, suggest that anchovy (sardine) flourishes in warm (cool) periods, consistent with previous results (Yasuda *et al.*, 1999); however, we were unable to assess the optimal temperature hypothesis proposed by Takasuka *et al.* (2007) using these linear functions. Regression analyses were then performed using quadratic functions, requiring them to be convex to define the optimal temperature. The best regression for anchovy was found using EWMET in days 5–15 ($R^2 = 0.40$, $P < 0.01$) with an optimal temperature of 22.3°C; the regressions from days 0–10 to days 25–35 were also significant ($R^2 = 0.23–0.40$, $P = 0.003–0.05$). The regression for sardine was not statistically significant.

Because of the spatial elasticity of the spawning ground with fluctuations in stock abundance, EWMET in the initial stage (mean of days 0–10) showed a significant correlation with spawning stock biomass: negative for anchovy ($r = -0.61$, $P < 0.01$) and positive for sardine ($r = 0.36$, $P = 0.07$). The correlation between SSB and LNRPS for anchovy was also significant. Note that the SSB contribution to LNRPS was not statistically significant for sardine over the period 1978–2004 (the period of transport examined in this study), whereas it was significant over the period 1950–2000 (Yatsu *et al.*, 2005).

The effects of EWMET averaged for all individuals from all SAs (EWMET-ALL) cannot be distinguished

	Days	<i>a</i>	T_o	<i>b</i>	R^2	<i>P</i>
Anchovy						
Linear	0–10	0.17 (0.43)	–	1.8	0.20	0.02
Quadratic	5–15	–0.093 (–0.64)	22.4	–45	0.40	<0.01
Sardine						
Linear	0–10	–0.39 (–0.35)	–	9.8	0.12	0.08

**a* and *b*, regression coefficients; T_o , optimal temperature; Days, the days elapsed since particle release; R^2 , determination coefficient; *P* significance level for the *F* test. Numbers in brackets indicate standardized partial regression coefficients tested using the *t* test. Note that we only show those regressions that exhibit the largest determination coefficient among 19 elapsed day bands and that satisfy both the *F* test and *t* test. See the text for further details.

Table 1. Summary of regression analyses of LNRPS on EWMET averaged for all areas (EWMET-ALL), using either a linear function, $LNRPS = a < T(t) > + b$, or a quadratic function, $LNRPS = a < (T(t) - T_o)^2 > + b^*$.

from those of SSB (density effect) for anchovy because of their close relationship, even though the dependence of growth rate on temperature (Takasuka *et al.*, 2007) implies its impact on RPS. A fundamental cause of this correlation is the correlation between SSB and egg abundance in the extended spawning grounds. Therefore, we performed a regression analysis using the EWMET of individuals from a single spawning area (EWMET-SA) that did not correlate with SSB, rather than using EWMET-ALL. SSB included the effects of the EWMET variability caused by expansion and contraction of the spawning ground.

Whereas the effects of EWMET-SA for all eight areas on LNRPS were examined separately, regressions with significant partial regression coefficients were found for one or two SAs for either linear or quadratic function (see Table 2). Because the contribution of SSB to LNRPS was not significant for sardine during 1978–2004, the coefficient of SSB was assumed to be the same as that given by Yatsu *et al.* (2005). Although SSB alone gave a significant regression for the anchovy LNRPS, significant improvements were achieved with linear and quadratic functions for EWMET-SA. A negative partial regression coefficient was found for a linear function of EWMET for individuals from SA3 (EWMET-SA3) on days 65–75 (partial regression coefficients were significant from days 60–70 to days 70–80), and an optimal temperature of 21.2°C was found with a quadratic function for EWMET-SA2 on days 5–15 (also significant on days 0–10). A significant regression was found for the

sardine with a linear function using EWMET-SA3 on days 25–35 (significant from days 20–30 to days 30–40), which had a negative partial regression coefficient; however, no significant convex quadratic function was found.

These analyses using EWMET-SA were based on the sites where spawning occurred each year; however, it is worth mentioning that a significant regression for sardine LNRPS with a remarkably higher determination coefficient was found with EWMET-SA5 on days 20–30 ($R^2 > 0.2$ from days 10–20 to days 40–50) for the sardine for years other than 1995, 2000, and 2001, when no sardine eggs were found in SA5.

Figure 11 shows the interannual variability of EWMET-SA2 and EWMET-SA3 for anchovy and EWMET-SA3 and EWMET-SA5 for sardine. The increasing trends for anchovy EWMET-SA3, sardine EWMET-SA3, and sardine EWMET-SA5, and the shift in the fluctuation range for anchovy EWMET-SA2 to 20–22°C after 1990, correspond to RPS variability (Fig. 2). As shown in Fig. 12, consideration of EWMET-SA improved the regression, especially for years with high variability. Further interpretations are made in the following section.

DISCUSSION AND CONCLUSIONS

The results of the regression analyses of EWMET-ALL and EWMET-SA obtained from particle-tracking experiments are basically consistent with the results of previous studies that examined the effects of temper-

Table 2. Summary of regression analyses of LNRPS on SSB and EWMET of single areas (EWMET-SA), using either a linear function, $LNRPS = a_{k0} < T(t) > + b_{k0} + \alpha$ SSB, or a quadratic function, $LNRPS = a_{k0} < (T(t) - T_o)^2 > + b_{k0} + \alpha$ SSB*.

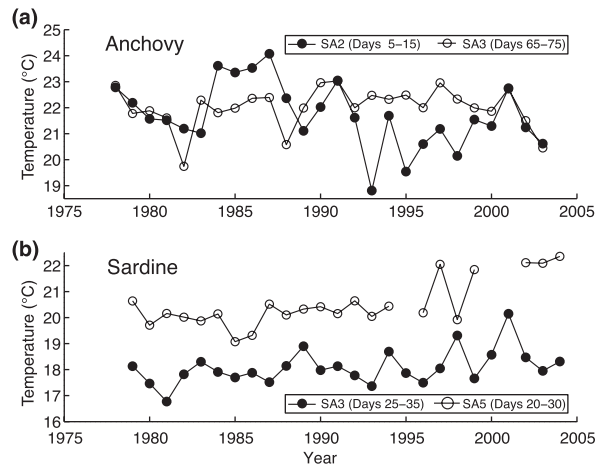
	SA	Days	α	a_{k0}	T_o	b_{k0}	R^2	P
Anchovy								
SSB	–	–	-1.5×10^{-3} (–0.73)	–	–	6.0	0.53	<0.01
SSB + Linear	SA3	65–75	-1.4×10^{-3} (–0.70)	–0.18 (–0.25)	–	10	0.59	<0.01
SSB + Quadratic	SA2	5–15	-1.5×10^{-3} (–0.73)	–0.057 (–0.36)	21.2	6.7	0.66	<0.01
Sardine								
SSB	–	–	$-1.7 \times 10^{-3}\dagger$	–	–	3.3	–	–
SSB + Linear	SA3	25–35	$-1.7 \times 10^{-3}\dagger$	–0.72 (–0.41)	–	16	0.18	0.03
SSB + Linear‡	SA5	20–30	$-1.7 \times 10^{-3}\dagger$	–0.78 (–0.61)	–	19	0.28	<0.01

* a and b , regression coefficients; T_o , optimal temperature; Days, the days elapsed since particle release; R^2 , determination coefficient; P significance level for the F test. Numbers in brackets indicate standardized partial regression coefficients tested using the t test. Note that we only show those regressions that exhibit the largest determination coefficient among 19 elapsed day bands and that satisfy both the F test and t test. See the text for further details.

$\dagger \alpha = -1.7 \times 10^{-3}$ (Yatsu *et al.*, 2005) was used as the partial regression coefficient, which was not significant for the data for 1978–2004 used in this study.

\ddagger Analysis was performed for the data (omitting the years 1995, 2000, and 2001) when no eggs were collected in SA5.

Figure 11. Interannual variations in the mean environmental temperatures of individuals from specific spawning areas, for (a) anchovy and (b) sardine, for which we found significant regression, as listed in Table 2.



ature on recruitment rates in anchovy and/or sardine using either linear or quadratic functions. A negative correlation was found between LNRPS and EWMET-ALL, EWMET-SA3, and EWMET-SA5 for sardine, as reported by Noto and Yasuda (1999) and Yatsu *et al.* (2005), who used the spatial mean temperature of KESA. The KESA temperature is considered to be a good representation of the environmental temperature of the sardine larvae transported to the Kuroshio Extension, especially in years of high stock abundance,

as a high determination coefficient was found with EWMET-SA5 (EWMET from the western part of the Kuroshio area) on days 20–30, the period in which the larvae and eggs are expected to be transported mainly to the Kuroshio Extension area (Itoh and Kimura, 2007). The impact of sardine larvae from SA5 on survival rates is also partly compatible with the suggestion by Kasai *et al.* (1997) that juveniles surviving in the areas east of Japan contribute to the recruitment of sardine, although their implication of the effect of the southward intrusion of the Oyashio was not evident in our study because an increase in egg production in SA5 (Fig. 7) mainly increased the transport toward DA2 and DA4 (Fig. 9), distant from the Oyashio.

Assuming a quadratic function, we found the optimal temperature for the anchovy, estimated with EWMET-ALL and EWMET-SA2, to be about 21–22°C, consistent with the results of the otolith analysis undertaken by Takasuka *et al.* (2007). Whereas the retrospective analyses of Takasuka *et al.* (2007) found a weak regression for anchovy LNRPS on spawning-ground temperature weighted by mean egg abundance, the significance was improved by using EWMET-ALL on days 5–15 or EWMET-SA2 on days 5–15 with SSB for the anchovy.

Because SSB variability also influences the timing of the spawning season in addition to spatial fluctuations in the extent of spawning grounds (Figs 6 and 7), EWMET-SA obtained by averaging over months are

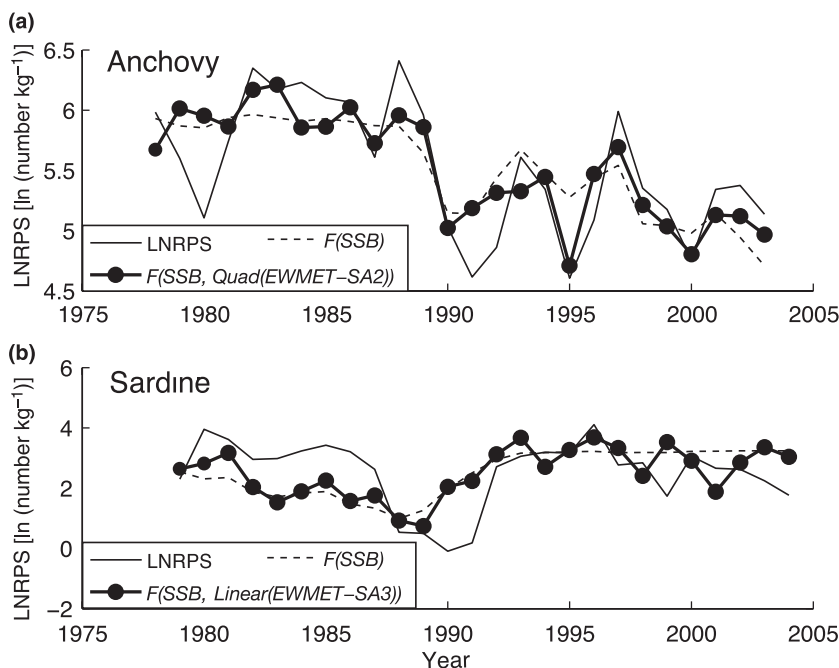


Figure 12. Interannual variations in observed LNRPS (solid lines) and its regression with SSB alone [dashed lines, denoted by $F(SSB)$] and with SSB and EWMET-SA [solid circles with lines, denoted by $F(SSB)$, $Quad$ (EWMET-SA2) for anchovy and $F(SSB)$, $Linear$ (EWMET-SA3) for sardine; quad and linear indicate quadratic and linear functions, respectively] for (a) anchovy and (b) sardine.

not necessarily independent of SSB. Hence, few EWMET-SA were statistically significant with SSB: only linear functions of EWMET-SA3 and quadratic functions of EWMET-SA2 were statistically significant for anchovy, and linear functions of EWMET-SA2 for sardine (EWMET-SA5 is not included because spawning did not occur every year in SA5) (Table 2). As moderate levels of egg abundance are maintained in SA2 for anchovy and SA3 for sardine even during times of low stock abundance, these areas are regarded as the core spawning grounds of anchovy and sardine, respectively. The role of SA3 in anchovy recruitment was unclear, because far fewer anchovy eggs are spawned there than at SA2.

The finding of significant and high determination coefficients with EWMET-ALL and EWMET-SA for anchovy and sardine during the initial stage (typically until day 30) relative to the later stage indicates the greater importance of the initial stage in terms of recruitment success. However, this does not signify the insignificance of the later stage, primarily because EWMET include contributions of all particles, irrespective of their environmental history: heavy mortality during the initial stage induced by environmental mismatch could cause noise in the regression analysis performed using EWMET of the later stages. The swimming of larvae, which was not included in the model, could also potentially contribute to any errors in the simulation.

In the regression analysis for anchovy using linear functions of EWMET-ALL, a significant negative relationship was detected in the later stage (after days 75–85) in addition to the positive relationship (which yielded the highest determination coefficient) observed during the initial stage. However, anchovy EWMET-ALL after days 75–85 showed a significant negative correlation with that on days 0–10 ($r = -0.47$, $P = 0.02$ on days 80–90). This finding is explained by the fact that anchovy spawning takes place in early summer: a relatively early (late) spawning season results in a cold (warm) environment during the initial stages and a warm (cold) environment after 3 months, during early autumn (Figs 7 and 10). Thus, the negative relationship after days 75–85 partly reflects the indirect, lingering influence of the initial stage; however, the possibility of direct effects is not rejected because EWMET-SA3 made a similar contribution to anchovy LNRPS but was insignificant during the initial stage.

Although we found a significant positive correlation between anchovy LNRPS and EWMET, including an implicit correlation between LNRPS and SSB, the significant negative standardized partial regression

coefficient obtained for the quadratic term suggests that the core range of the optimal temperature is just slightly higher than that of the egg density-weighted mean habitat temperature for the eggs and larvae of anchovy. Conversely, sardine LNRPS were regressed significantly only by linear functions of EWMET, suggesting that the core range of the optimal temperature is lower than that of the egg-density-weighted mean habitat temperature of the sardine eggs and larvae. This finding arises partly because the warm spawning grounds of sardine correspond to those formed in the Kuroshio area, especially when stock abundance is high. The habitat temperature averaged without weighting is lower than that averaged with weighting, and is close to the optimal temperature reported by Takasuka *et al.* (2008). It seems that the mean environmental temperature of sardine without weighting, which implicitly assumes the importance of inshore and coastal areas, is close to the core habitat temperature range; however, we were unable to define the optimal temperature, even using EWMET of SA3 (EWMET-SA3), which is regarded in this study as the core spawning ground.

Thus, the differences in stock variability between anchovy and sardine cannot be explained solely in terms of their habitats or optimal temperatures: their responses to environmental fluctuations must also be taken into account. Larger numbers of anchovies survive in coastal waters where the degree of environmental variability is moderate, whereas sardines take advantage of offshore waters where environmental variability is high, but where the total carrying capacity is also high. These different strategies may also be related to differences in basic biology, such as the high and low spawning frequencies and egg productions of anchovy and sardine, respectively (Kuroda, 1991; Tsuruta, 1992).

The above hypothesis regarding the contrasting strategies of the two species does not contradict previous hypotheses (Noto and Yasuda, 1999; Yatsu *et al.*, 2005; Takasuka *et al.*, 2007); rather, it combines them. The more pronounced nature of fluctuations in abundance in sardines than in anchovies can also be explained by this hypothesis. Because the main habitat area of the northern anchovy (*Engraulis mordax*) in the California Current system is distributed predominantly in relatively coastal waters compared with that of the Pacific sardine (*Sardinops sagax*) (Checkley *et al.*, 2000), the synchronous anchovy–sardine cycles on both sides of the North Pacific can be explained by the contrasting environmental effects on coastal and offshore waters of large-scale climate change, such as the Pacific Decadal Oscillation.

In this study, particle-tracking experiments were performed to investigate the transport and Lagrangian temperature variability experienced by eggs and larvae of the Japanese anchovy and Japanese sardine, and to examine the effects of this variability on recruitment rates. We found that the contribution of environmental temperature to LNRPS is significant for both the anchovy and sardine; density effects represented by SSB are also important, especially for the anchovy. Despite the fact that SSB shows a close relationship with EWMET via the spatial distribution of eggs, we successfully separated the two effects using the EWMET of single spawning grounds considered to be the core spawning grounds: SA2 (eastern coastal area south of Japan) for the anchovy and SA3 (western inshore area south of Japan) for the sardine. Whereas the anchovy response to environmental temperature was quadratic, with an optimal temperature of 21–22°C, the sardine response was linear, with a negative regression coefficient. This finding suggests that the survival strategies of the anchovy make it suitable for a moderate coastal environment, whereas those of the sardine take advantage of the offshore environment.

ACKNOWLEDGEMENTS

We thank members of the OFES group for providing model outputs, and Drs Oozeki and Takasuka and all those involved in field sampling undertaken by the Fisheries Agency of Japan for providing egg production data. Dr Yatsu kindly provided historical landing data. Finally, we extend our thanks to two anonymous reviewers and the journal editor for their valuable comments.

REFERENCES

- Anonymous (1997–2004) *Annual Meeting Report of Egg and Larval Survey of Small Pelagic Fish off the Pacific Coast of Japan*, No. 17–24 (in Japanese). Tokyo: Fisheries Research Agency of Japan.
- Asselin, R. (1972) Frequency filter for time integrations. *Mon Weather Rev.* **100**:487–490.
- Chavez, F.P., Ryan, J., Lluch-Cota, S.E. and Niquen, M. (2003) From anchovies to sardines and back: multidecadal change in the Pacific Ocean. *Science* **299**: 217–221.
- Checkley, D.M., Dotson, R.C. and Griffith, D.A. (2000) Continuous, underway sampling of eggs of Pacific sardine (*Sardinops sagax*) and northern anchovy (*Engraulis mordax*) in spring 1996 and 1997 off southern and central California. *Deep-Sea Res. Pt II* **47**:1139–1155.
- Hare, S.R. and Mantua, N.J. (2000) Empirical evidence for North Pacific regime shifts in 1977 and 1989. *Prog. Oceanogr.* **47**:103–145.
- Heath, M., Zenitani, H., Watanabe, Y., Kimura, R. and Ishida, M. (1998) Modelling the dispersal of larval Japanese sardine, *Sardinops melanostictus*, by the Kuroshio current in 1993 and 1994. *Fish. Oceanogr.* **7**:335–346.
- Hjort, J. (1914) Fluctuation in the great fisheries of northern Europe viewed in the light of biological research. *Rapp. PV Reun. Cons. Perm. Int. Explor. Mer.* **20**:1–228.
- Ishida, M. and Kikuchi, H. (1992) *Monthly Egg Productions of the Japanese Sardine, Anchovy, and Mackerels of the Southern Coast of Japan by Egg Censuses: January 1989 through December 1990*, 86 pp (in Japanese with English abstract). Tokyo: Japan Fisheries Agency.
- Itoh, S. and Kimura, S. (2007) Transport and survival of larvae of pelagic fishes in Kuroshio system region estimated with Lagrangian drifters. *Fish. Sci.* **73**:1295–1308.
- Kasai, A., Kishi, M.J. and Sugimoto, T. (1992) Modeling the transport and survival of Japanese sardine larvae in and around the Kuroshio current. *Fish. Oceanogr.* **1**:1–10.
- Kasai, A., Sugimoto, T. and Nakata, H. (1997) The dependence of yearly recruitment of Japanese sardine *Sardinops melanostictus* on survival in the Kuroshio–Oyashio Transition region. *Fish. Sci.* **63**:372–377.
- Kawai, H. (1969) Statistical estimation of isotherms indicative of Kuroshio axis. *Deep-Sea Res.* **16**:109–115.
- Kawasaki, T. (1991) Long-term variability in the pelagic fish populations. In: *Long-Term Variability of Pelagic Fish Populations and their Environment*. T. Kawasaki, S. Tanaka, Y. Toba & A. Taniguchi (eds) Oxford: Pergamon Press, pp. 47–60.
- Kikuchi, H. and Konishi, Y. (1990) *Monthly Egg Productions of the Japanese Sardine, Anchovy, and Mackerels of the Southern Coast of Japan by Egg Censuses: January 1987 through December 1988*, 72 pp (in Japanese with English abstract). Tokyo: Japan Fisheries Agency.
- Kubota, H., Oozeki, Y., Ishida, M. et al. (1999) Distributions of Eggs and Larvae of Japanese Sardine, Japanese Anchovy, Mackerels, Round Herring, Jack Mackerel and Japanese Common Squid in the Waters around Japan, 1994 through 1996, 352 pp (in Japanese with English abstract). Yokohama: National Research Institute of Fisheries Science.
- Kuroda, K. (1991) Studies on the recruitment process focusing on the early life history of the Japanese Sardine, *Sardinops melanostictus* (Schlegel). *Bull. Natl. Res. Inst. Fish. Sci.* **3**:25–278.
- Lluch-Belda, D., Crawford, R.J.M., Kawasaki, T. et al. (1989) Worldwide fluctuations of sardine and anchovy stocks – the regime problem. *S. Afr. J. Mar. Sci.* **8**:195–205.
- Mantua, N.J., Hare, S.R., Zhang, Y., Wallace, J.M. and Francis, R.C. (1997) A Pacific interdecadal climate oscillation with impacts on salmon production. *Bull. Am. Meteorol. Soc.* **78**:1069–1079.
- Marine Information Research Center, Japan Hydrographic Association (2007) *Data Sets of the Axis of the Kuroshio from 1955 to 2006*. CD-ROM. Japan Hydrographic Association, Japan Hydrographic Association.
- Masumoto, Y., Sasaki, H., Kagimoto, T. et al. (2004) A fifty-year eddy-resolving simulation of the world ocean – preliminary outcomes of OFES (OGCM for the Earth Simulator). *J. Earth Sim.* **1**:35–56.
- Mori, K., Kuroda, K. and Konishi, Y. (1988) *Monthly Egg Productions of the Japanese Sardine, Anchovy, and Mackerels off the Southern Coast of Japan by Egg Censuses: January 1978 through*

- 1986, 321 pp. Tokyo: Tokai Regional Fisheries Research Laboratory.
- Nagasawa, K. and Davis, N.D. (1998) Easternmost records for the distribution of Japanese anchovy (*Engraulis japonicus*). *Bull. Japan. Soc. Fish. Oceanogr.* **62**:176–180.
- Nishida, H. (2005) Stock assessment and ABC calculation for Japanese sardine (*Sardinops melanostictus*) in the northwestern Pacific under Japanese TAC system. *Global Environ. Res.* **9**:125–129.
- Nishikawa, H. and Yasuda, I. (2008) Japanese sardine (*Sardinops melanostictus*) mortality in relation to the winter mixed layer depth in the Kuroshio Extension region. *Fish. Oceanogr.* **17**:411–420.
- Nonaka, M., Nakamura, H., Tanimoto, Y., Kagimoto, T. and Sasaki, H. (2006) Decadal variability in the Kuroshio–Oyashio Extension simulated in an eddy-resolving OGCM. *J. Climate* **19**:1970–1989.
- Noto, M. and Yasuda, I. (1999) Population decline of the Japanese sardine, *Sardinops melanostictus*, in relation to sea surface temperature in the Kuroshio Extension. *Can. J. Fish. Aquat. Sci.* **56**:973–983.
- Oozeki, Y., Kubota, H., Takasuka, A., Akamine, T. and Shimizu, A. (2005) Stock assessment and evaluation for the Pacific stock of Japanese anchovy (fiscal year 2005). In: *Marine Fisheries Stock Assessment and Evaluation for Japanese Waters (Fiscal Year 2005/2006)*. Tokyo: Fisheries Agency and Fisheries Research Agency of Japan, pp. 604–628.
- Sasaki, H., Nonaka, M., Masumoto, Y., Sasai, Y., Uehara, H. and Sakuma, H. (2008) An eddy-resolving hindcast simulation of the quasi-global ocean from 1950 to 2003 on the Earth Simulator. In: *High Resolution Numerical Modelling of the Atmosphere and Ocean*. K. Hamilton & W. Ohfuchi (eds) New York: Springer, pp. 157–185.
- Sugisaki, H. (1996) Distribution of larval and juvenile Japanese sardine (*Sardinops melanostictus*) in the western North Pacific and its relevance to predation of these stages. In: *Survival Strategies in Early Life Stages of Marine Resources*. Y. Watanabe, Y. Yamashita & Y. Oozeki (eds) Rotterdam: Balkema, pp. 261–270.
- Taguchi, B., Xie, S.-P., Schneider, N., Nonaka, M., Sasaki, H. and Sasai, Y. (2007) Decadal variability of the Kuroshio extension: observations and an eddy-resolving model hindcast. *J. Climate* **20**:2357–2377.
- Takasuka, A., Oozeki, Y. and Aoki, I. (2007) Optimal growth temperature hypothesis: why do anchovy flourish and sardine collapse or vice versa under the same ocean regime? *Can. J. Fish. Aquat. Sci.* **64**:768–776.
- Takasuka, A., Oozeki, Y., Kubota, H. and Lluch-Cota, S.E. (2008) Contrasting spawning temperature optima: why are anchovy and sardine regime shifts synchronous across the North Pacific? *Prog. Oceanogr.* **77**:225–232.
- Tsuruta, Y. (1992) Reproduction in the Japanese anchovy (*Engraulis japonica*) as related to population fluctuation. *Bull. N.R.I.F.E.* **13**:129–168.
- Watanabe, Y., Zenitani, H. and Kimura, R. (1995) Population decline of the Japanese sardine *Sardinops melanostictus* owing to recruitment failures. *Can. J. Fish. Aquat. Sci.* **52**:1609–1616.
- Watanabe, Y., Zenitani, H. and Kimura, R. (1996) Offshore expansion of spawning of the Japanese sardine, *Sardinops melanostictus*, and its implication for egg and larval survival. *Can. J. Fish. Aquat. Sci.* **53**:55–61.
- Yasuda, I., Sugisaki, H., Watanabe, Y., Minobe, S.S. and Oozeki, Y. (1999) Interdecadal variations in Japanese sardine and ocean/climate. *Fish. Oceanogr.* **8**:18–24.
- Yatsu, A., Watanabe, T., Ishida, M., Sugisaki, H. and Jacobson, L.D. (2005) Environmental effects on recruitment and productivity of Japanese sardine *Sardinops melanostictus* and chub mackerel *Scomber japonicus* with recommendations for management. *Fish. Oceanogr.* **14**:263–278.
- Zenitani, H., Ishida, M., Konishi, Y., Goto, T., Watanabe, Y. and Kimura, R. (1995) *Distributions of Eggs and Larvae of Japanese Sardine, Japanese Anchovy, Mackerels, Round Herring, Jack Mackerel and Japanese Common Squid in the Waters around Japan, 1991 through 1993*. 368 pp (in Japanese with English abstract). Tokyo: Japan Fisheries Agency.